Nanoscale Advances

ROYAL SOCIETY OF CHEMISTRY

PAPER

View Article Online
View Journal | View Issue

Cite this: *Nanoscale Adv.*, 2023, **5**, 2547

Additive manufacturing of eco-friendly building insulation materials by recycling pulp and paper†

Meng-Lun Lee, ‡[a] Arpita Sarkar,‡[a] Zipeng Guo, [b] Chi Zhou,[b] Jason N. Armstrong[a] and Shenqiang Ren *[acd]

Received 17th January 2023
Accepted 6th April 2023

DOI: 10.1039/d3na00036b

rsc.li/nanoscale-advances

Thermal insulation materials by recycling pulp and paper wastes play an important role in environmental sustainability of green buildings. As society is pursuing the goal of zero carbon emissions, it is highly desirable to use eco-friendly materials and manufacturing technologies for building insulation envelopes. Here we report additive manufacturing of flexible and hydrophobic insulation composites from recycled cellulose-based fibers and silica aerogel. The resultant cellulose-aerogel composites exhibit thermal conductivity of 34.68 mW m^{-1} K^{-1}, mechanical flexibility with a flexural modulus of 429.21 MPa, and superhydrophobicity with water contact angle of 158.72°. Moreover, we present the additive manufacturing process of recycled cellulose aerogel composites, providing enormous potential for high energy efficiency and carbon-sequestration building applications.

Introduction

The demand for cellulose-based insulation is growing continuously while sustainability in its production becomes the primary concern regarding fossil fuel consumption and chemical waste.[1] Cellulose is one of the most abundant polymers as a structural component of carbon-storing natural plants, which is also a viable alternative to fossil fuel-derived materials.[2] Apart from natural sources like plants or wood, cellulose fibers can be obtained from recycling pulp or paper waste.[3,4] Recycling one ton of pulp paper could be equivalent to saving 17 trees, 3.3 cubic yards of landfill space, 360 and 100 gallons of water and gasoline, as well as 10 megawatts of electricity.[5] Therefore, recycling pulp and paper instead of landfill could be a new value-added application of cellulose-based insulation materials. Moreover, unlike petroleum-based insulation materials, recycled cellulose materials do not rely on non-renewable resources and produce chemical waste and pollution in the manufacturing process.[6] However, the low-performing characteristics of cellulose such as low thermal and mechanical performance, and hygroscopicity restricts its potential for the development of cellulose-based building insulation materials.[7]

Along with the eco-friendly strategy of producing recycled materials, a cost-effective manufacturing process with low environmental impacts is required. Additive manufacturing (AM), also known as 3D printing, can add enormous value to the production of carbon-storing and carbon-negative products through on-demand manufacturing, zero-waste fabrication, and shortening supply chains.[8] Different from the conventional manufacturing of subtracting materials from the building block, AM assembles the printable materials in a layer-by-layer fashion without wasting raw materials, thus making AM an eco-friendly manufacturing process.[9,10] However, challenges such as preparing the printable materials and reliable manufacturing process are bottlenecks of 3D printing the recycled cellulose pulp and paper.

Here, to enhance the mechanical strength and thermal insulation behavior of recycled cellulose fibers, we introduce superinsulation silica aerogel for the additive manufacturing of recycled cellulose aerogel composite materials. Incorporating cellulose fibers with silica aerogel,[11–13] could also compensate for the effect of fragility, while delivering high mechanical strength and thermal insulation properties.[14] We report both one-step precursor gelation (*in situ*) and two-step physical mixing for the manufacturing of flexible and superhydrophobic cellulose-aerogel composites, with the capability of additive manufacturing through extrusion-based 3D printing. The *in situ* method presents the formation of cross-linked structure which significantly improves the mechanical strength of the composites, while exhibiting thermal conductivity of 34.68 mW m^{-1} K^{-1}, a flexural modulus of 429.21 MPa, and hydrophobicity with

[a]*Department of Mechanical and Aerospace Engineering, University at Buffalo, The State University of New York, Buffalo, New York 14260, USA. E-mail: shenren@buffalo.edu*

[b]*Department of Industrial and Systems Engineering, University at Buffalo, The State University of New York, Buffalo, New York 14260, USA*

[c]*Department of Chemistry, University at Buffalo, The State University of New York, Buffalo, NY 14260, USA*

[d]*Research and Education in Energy, Environment & Water (RENEW), University at Buffalo, The State University of New York, Buffalo, NY 14260, USA*

† Electronic supplementary information (ESI) available. See DOI: https://doi.org/10.1039/d3na00036b

‡ Equal contribution.

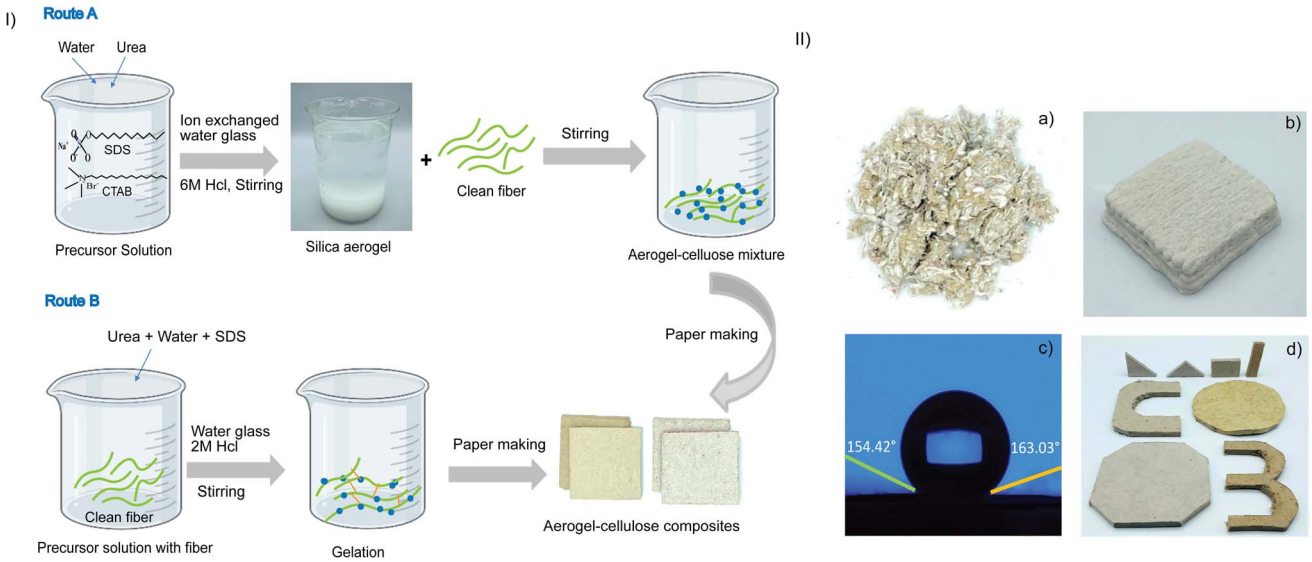

Fig. 1 (I) Schematic diagram of the *in situ* and physical mixing synthesis process of aerogel-cellulose composites, (II) (a) optical image of clean fiber, (b) 3D printing image of the composite, (c) image of the hydrophobic capability of the composite after trichlorosilane surface coating and (d) images showing different shapes and machinability of the aerogel-cellulose composite.

the water contact angle of 158.72°. We demonstrate 3D-printed insulation composites as the first attempt of using additive manufacturing technologies to fabricate recycled pulp and paper. The proposed additive manufacturing strategy provides a solution for efficient and flexible design, lower costs, and zero-waste production process.

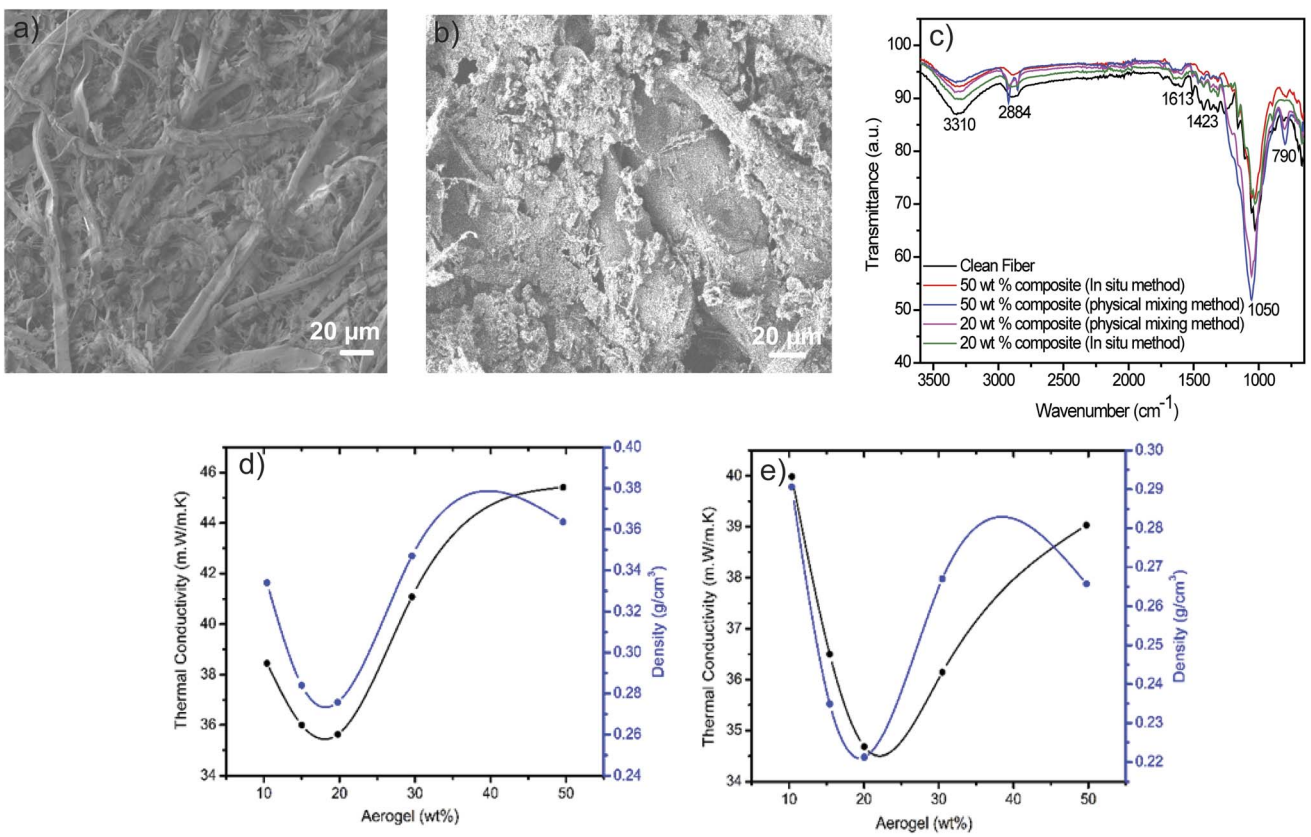

Fig. 2 (a) SEM images of 20 wt% cellulose-aerogel nanocomposites prepared from *in situ* method, (b) SEM images of 20 wt% cellulose-aerogel nanocomposites prepared from physical mixing method, (c) FTIR spectra of different wt% of cellulose-aerogel composite, (d and e) thermal conductivity *vs.* density plot for different wt% of the cellulose fiber reinforced aerogel nanocomposites prepared from *in situ* and physical mixing method respectively.

Results and discussion

Fig. 1 represents the schematic diagram of the physical mixing and the *in situ* methods for the manufacturing of recycled cellulose and aerogel composites. Route A shows the flowchart of the synthesis of the sodium-silicate-based aerogel *via* the physical mixing method. In this method, different concentrations of silica gel precursor are added with cellulose fibers for the preparation of the aerogel-cellulose composites under ambient pressure drying. For the *in situ* method as shown in route B, cellulose fibers are treated with the urea, sodium dodecyl sulfate (SDS), and water glass before the gelation to prepare the cellulose–silica gel precursor, which then undergoes a gelation process to enhance and maintain the 3D network. The gelation behavior in the aerogel cellulose composites is facilitated by its cross-linking nature. The aerogel is crosslinked by weak interactions through hydrogen bonds, van der Waals forces, or electrostatic interactions.[15–17] The *in situ* gelation of cellulose fiber-aerogel composite is resulted from synergistic complexation between cellulose fiber and silica network upon aging, possibly through hydrogen bonding between the free hydroxyls on the silica and hydroxyls group on the cellulose fiber. The as-synthesized fibrous cross-linked aerogel-cellulose composite not only can survive the subsequent ambient pressure drying process but also improve the mechanical properties of the composites. The aerogel-cellulose composite exhibit superhydrophobicity, the capability of 3D printing, and machinability as shown in Fig. 1(II), and S1–S4.†

The structural and morphological features of as prepared aerogel-cellulose composites are studied using scanning electron microscopy (SEM, Fig. 2a and b). The SEM images for the *in situ* method (Fig. 2a and S5†) show a highly porous crosslinked structure where aerogel consists of an interconnected network with cellulose fibers and the fibers having a rod-like structure with an average diameter of 45–120 μm to form an open pores network. The aerogel-cellulose composite with a crosslinked

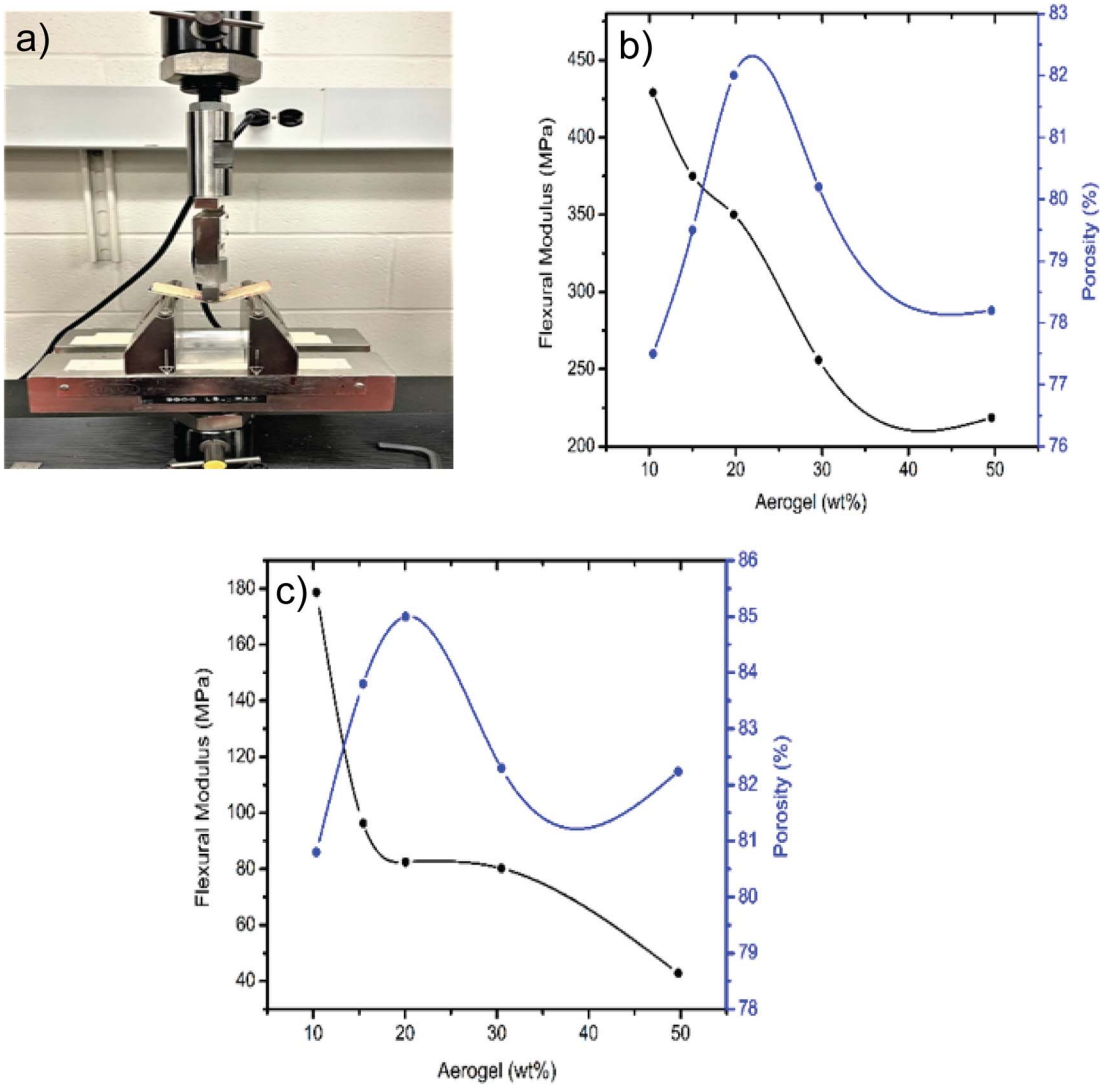

Fig. 3 (a) Three-point bending test of the composites, (b and c) porosity *vs.* flexural modulus plot for different concentrations of the cellulose fiber reinforced aerogel nanocomposites prepared from *in situ* and physical mixing method respectively.

structure can be formed *via in situ* method due to the production of material in the gel framework of cellulose fibers. On the other hand, the SEM images of cellulose-aerogel composite in the case of the physical mixing show hierarchically porous structures (Fig. 2b) and the formation of aggregation which increases upon aerogel concentration from 10 to 50 wt% (Fig. S6†). Furthermore, Fourier-transform infrared spectroscopy (FTIR) has been used to evaluate the formation of aerogel-cellulose composites. Fig. 2c shows the FTIR spectra of composites prepared from the *in situ* and physical mixing methods. In the FTIR spectrum, the typical absorption peaks for cellulose were observed at 3310 cm^{-1} (O–H stretching), 2884 cm^{-1} (C–H symmetric stretching), 1423 cm^{-1} (–CH_2 stretching), 1365 cm^{-1} (–CH stretching) and 1332 cm^{-1} (C–O stretching). The peaks at 1632 cm^{-1} represent the vibration of H_2O molecules absorbed in cellulose. Moreover, the peaks at 3313 and 1160 cm^{-1} in the aerogel-cellulose composite related to the overlapping effect between cellulose and silica which corresponds to the O–H stretching vibration and Si–O–Si asymmetric stretching vibration respectively, and indicate that silica is impregnated into the aerogel-cellulose composites. On the other hand, a peak around 790 cm^{-1} resulted from Si–O–Si symmetric vibration along with an adjacent peak at 960 cm^{-1} for rocking bending vibrations of the Si–OH group in the case of the *in situ* method indicates the cross-linking nature between the SiO_2 and cellulose fibers in the aerogel-cellulose composites Fig. 2d and e reveal the change in the thermal conductivity with increasing aerogel wt% in the cellulose fiber composites. As increasing aerogel up to 20 wt% in both methods, thermal conductivity has been decreased and reaches 35.2 mW m^{-1} K^{-1} for the *in situ* and 34.68 mW m^{-1} K^{-1} for physical mixing method. It is interesting to note that thermal conductivity increases after increasing the aerogel above 20 wt%. The reason behind this phenomenon is when the aerogel concentration increases from 0 to 20 wt% its leads to lower density and higher porosity resulting lower thermal conductivity (Fig. 2d and e). However, increasing the aerogel concentration beyond 20 wt%, the aggregated microstructure leads to a decrease in porosity and an increase of density resulting in higher thermal conductivity (Fig. S5 and S6†). The thermal insulation property of the as-prepared composite is better than few previously reported materials as shown in Table S1.†

The mechanical properties of the recycled cellulose aerogel composite immensely affect the application of building insulation materials. Fig. 3a–c shows the bending test and mechanical behavior of the composites prepared from the *in situ* and physical mixing methods. It is worth noting that the flexural modulus for the samples prepared from the *in situ* method (Fig. 3b) is higher (210–430 MPa) than that of the composites prepared from the physical mixing (40–180 MPa) (Fig. 3c). Moreover, the compression modulus is also higher in case of the *in situ* method than the physical mixing method as shown in Fig. S7.† This is mainly due to the crosslinking behavior in the *in situ* method which forms a robust structure and significantly improves the mechanical strength of the composites.

Hydrophobicity is another key factor for cellulose based building insulation materials. The surface wettability of trichloro silane coated cellulose reinforced aerogel composite is

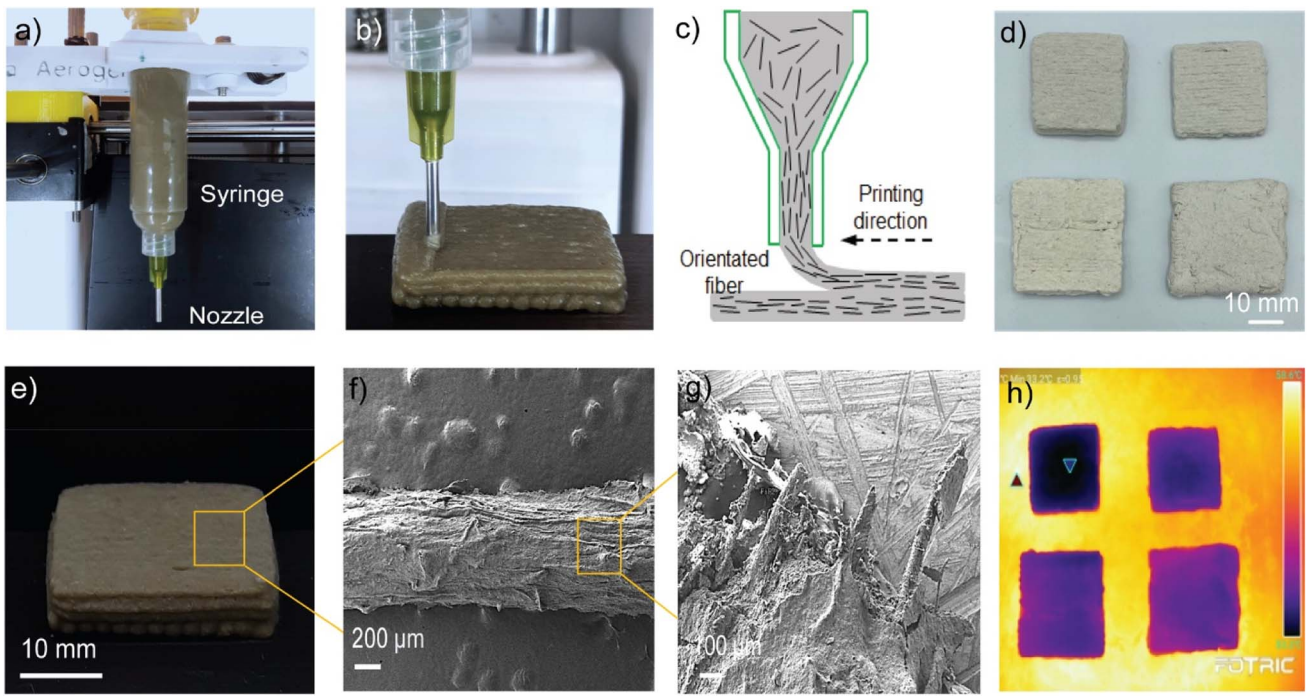

Fig. 4 Additive manufacturing of recycled cellulose pulp and paper. (a) Photograph of extrusion-based 3D printing setup, (b) close-up view at the nozzle region, (c) schematic diagram of fiber alignment during extrusion printing, (d) and (e) 3D-printed specimens with different thicknesses of the composites, (f) and (g) SEM images of 3D-printed composites, (h) thermal infrared (IR) image of the thermal insulation under 60 °C thermal heating.

studied by water contact angle measurement, shown in Fig. S8.† Fig. S8a† reveals when the water droplet comes into contact with the composite without surface treatment, the droplet is absorbed instantly suggesting its hydrophilic nature due to the presence of a large number of hydroxyl groups in cellulose. On the other hand, surface treated composite shows a water contact angle of 152.78° which indicates the aerogel-cellulose composite of a highly hydrophobic surface after trichloro silane treatment (Fig. S8b†). The humidity-dependent thermal insulation test using a programmable humidity and temperature chamber is shown in Fig. S8c.† Fig. S8c† revealed the comparison of increment of thermal conductivity values of composites with and without surface treatment, while a higher increase in thermal conductivity (18% increase) is shown in the composite without surface treatment. The surface-treated composite displays a change in the thermal conductivity of around 4%, which implies that the hydrophobic treatment of the aerogel-cellulose composite could significantly affect its water absorption capacity.

Rapid prototyping of thermal insulation composite plays an important role in building applications. A pneumatic pressure-based extrusion printing setup is used for printing the recycled cellulose and aerogel composites. The prepared ink is loaded into a 10 cc syringe barrel and mounted onto a customized 3-axis printer platform as shown in Fig. 4a, while an air pressure regulator is connected to the syringe barrel and controls the extrusion pressure. The printing flow speed and the layer height are 10 mm s^{-1} and 0.8 mm, respectively. The ink is subjected to a shear pressure during the printing, as the ink is printed along the lateral path (Fig. 4b and c), shear pressure orientates the fiber in the lateral direction. The SEM images in Fig. 4f and g reveals the orientated fibers. Fig. 4d and e shows the 3D-printed insulation composites with different thicknesses. Fig. 4h shows the top surface temperature of thermal insulation composites under 60 °C heating. Under the same temperature, specimens with different thicknesses have a noticeable temperature difference, and the top surface temperature decreases when the sample thickness increases. Moreover, the composites with aerogel with the same thickness exhibit a higher top surface temperature than the non-aerogel sample, indicating a better thermal performance. This is the first attempt of using additive manufacturing technology to fabricate recycled cellulose pulp and paper. The future efforts will be focused on improving the shape fidelity of the printed specimen and increasing the throughput of thermal insulation composites.

Conclusion

We report the manufacturing of aerogel-containing recycled cellulose insulation composites. The *in situ* method shows the formation of crosslinked aerogel-cellulose nanostructure which significantly improves the mechanical strength of the composites compared to the physical mixing method. The as-prepared fiber-aerogel composite exhibits a thermal conductivity of 34.68 mW m^{-1} K^{-1}, a flexural modulus of 429.21 MPa, and super-hydrophobicity with the water contact angle of 158.72°. Due to the superior thermal conductivity performance, this highly porous, and super hydrophobic composite has the potential for versatile applications such as thermal insulating materials, mesoporous scaffolding, and oil adsorbents. Using additive manufacturing can fabricate cellulose composites with high efficiency, low costs and waste, providing an eco-friendly manufacturing process for future building envelop materials.

Experimental section

Chemicals and materials

The recycled cellulose fiber is acquired from the Clean Fiber. Urea and sodium dodecyl sulfate (SDS) are obtained from J. T. Baker. Sodium silicate solution (water glass) and hydrochloric acid (HCl) are purchased from Ward's Science and VWR Chemicals, respectively. Hexa-decyl trimethylammonium bromide (CTAB) and cation-exchange resin (Amberlite IRC120H, hydrogen form) are provided by Sigma-Aldrich. The hydrophobic coating is carried out by using 1*H*,1*H*,2*H*,2*H*-perfluorooctyltrichlorosilane (PFOTCS), 97%, purchased from Thermo Scientific.

Synthesis methods

Physical mixing method

Synthesis of the ion-exchange-sodium-silicate-based aerogel precursor. At first, 4.1 molar urea is added to 100 mL of DI water and then stirred for one hour until complete dilution. Next, SDS and CTAB with an 0.12 mol L^{-1} co-surfactant ratio are added to the urea-DI water mixture, followed by stirring for 2 hours until the solution becomes semi-transparent. Then, the ion-exchanged water glass, which has been prepared using the previously reported method[18] was added to the mixture at a 25 wt% proportion and stirred for at least 5 minutes until a homogeneous solution is achieved. Subsequently, HCl and DI water with a 1 : 2 volume-to-volume is added to the solution and then stirred for 5 minutes. Finally, the precursor is placed into a preheated oven at 80 °C for at least 24 hours until gelation is completed.

Synthesis of the aerogel-cellulose composite. Different wt% of aerogel-cellulose composites have been synthesized by varying aerogel concentrations into the precursor mixture. At first, the cellulose fiber is blended with 1 liter of de-ionized (DI) water. After that, the blended fiber is transferred to a large beaker and thoroughly mixed with the required volume of the aerogel using an overhead stirrer. Next, an additional volume of approximately 2 liter DI water is added to achieve adequate fiber dispersion. After that, a sample-making unit with vacuum filtration is used to process the fiber-aerogel slurry, and the resulting wet composite membranes are dried in a preheated oven at 60 °C for 24 to 48 hours. Multiple layers of metal mesh on both sides of the wet samples and additional load are applied during ambient drying to ensure the sample quality and increase the water removal rate.

In situ method

Synthesis of clean fiber-based silica aerogel precursor. In this process at first, 10 g of dried fibers were taken in a beaker and 100 mL of distilled water was added to it. After that, 1.0 g

sodium dodecyl sulfate (SDS) and 0.15 mol urea (9.0 g), were added and the mixture was stirred for 3 h to get a homogenous solution. Next, reagent-grade sodium silicate solution (11 mL) was added to the precursor mixture, followed by the addition of 2 M HCl until the pH of the solution becomes 9.0. After that, the solution mixture was kept in the oven at 60 °C for gelation.

Purification procedure. The cellulose fibers-based silica aerogel precursor was first taken into a beaker, and 2 L of DI water was added to it. After that, the precursor mixture was homogenized by using an overhead mechanical agitator and kept at 60 °C for phase separation. After the phase separation, the top layer was drained, and this process was repeated 4–5 times until a clear phase of water was obtained above the precursor mixture.

Synthesis of the aerogel-cellulose composite. For the synthesis of the aerogel-cellulose composite, 2 L of DI water was added to the cleaned aerogel precursor and mixed with an overhead mechanical agitator. Next, the homogenized solution was transferred to paper making setup. After that, the composite was taken out and kept between the perforated stainless sheets and kept drying inside a preheated oven at 60 °C.

3D-printing

Ink formulation. The 3D printable colloidal ink is prepared by mixing the aerogel and fiber suspension with a 2 wt% dispersing agent (propylene carbonate) at room temperature for 12 hours. Then the cellulose nanofiber is added to the ink at 1.5 wt% as a viscosity modifier, followed by 6 hour mixing using a blender (Cole-Parmer). Finally, the colloidal ink is degassed using a vacuum desiccator. All the chemicals are used as purchased without any modification.

Physical measurements. The density of the cellulose-aerogel composite is calculated from its weight-to-volume ratio. The microscopic morphology of the cellulose-aerogel specimen is observed using Carl Zeiss AURIGA scanning electron microscope (SEM). The Agilent Cary 630 Fourier-transform infrared spectroscopy (FTIR) spectrometer is used to investigate the chemical bonding of the cellulose-aerogel composite specimen. The thermal conductivity and the thickness of the composite membranes are measured using a heat flow meter from Thermtest HFM-100. Infrared images are captured using Fotric 225 Pro Thermal Camera.

In addition, the porosity of the cellulose-aerogel samples is calculated from bulk and skeletal densities following eqn (1):

$$\text{Porosity } (\%) = \left(1 - \frac{\rho_b}{\rho_s}\right) \times 100 \quad (1)$$

where ρ_b is the bulk density determined by weight-to-volume ratio and ρ_s is the skeletal density assessed with the pycnometry system Micromeritics Accu-Pyc II 1340.

Conflicts of interest

There are no conflicts to declare.

Acknowledgements

The information, data, or work presented herein was funded in part by the Advanced Research Projects Agency-Energy (ARPA-E), U.S. Department of Energy, under Award Number DE-AR0001630. The views and opinions of authors expressed herein do not necessarily state or reflect those of the United States Government or any agency thereof.

References

1 S. V. Ewijk, J. A. Stegemann and P. Ekins, *Nat. Sustain.*, 2021, **4**, 180–187.
2 M. John, A. S. Sarah, E. Eduardo, R. Antonio, R. Alejandro, L. Eneko, F. D. Ryan and D. R. Juan, *Appl. Sci.*, 2020, **1**, 65.
3 S. Vadahanambi and P. Hyun, *Materials*, 2020, **13**, 2850.
4 B. Medronho and B. Lindman, *Adv. Colloid Interface Sci.*, 2014, **222**, 1–7.
5 M. O. Rahman, M. Hannan, E. Scavino, A. Hussain and H. Basri, *Eur. J. Sci. Res.*, 2009, **25**, 96–103.
6 K. Wu, H. Wu, R. Wang, X. Yan, W. Sun, Y. Liu, Y. Kuang, F. Jiang and S. Chen, *Ind. Crops Prod.*, 2022, **177**, 114424.
7 S. Acharya, S. Liyanage, P. Parajuli, S. Rumi, J. L. Shamshina and N. Abidi, *Polymers*, 2021, **13**, 4344.
8 D. N. Tuan, K. Alireza, I. Gabriele, T. Q. N. Kate and H. David, *Composites, Part B*, 2018, **143**, 172.
9 K. P. Akhilesh, K. M. Amar and M. Manjusri, *RSC Adv.*, 2021, **11**, 36398.
10 A. S. Mauricio, E. R. Fernando, M. G. Carmen and R. H. Juan, *Polymers*, 2022, **14**, 1351.
11 H. M. Kim, Y. J. Noh, J. Yu, S. Y. Kim and J. R. Youn, *Composites*, 2015, **75**, 39–45.
12 J. Cho, H. G. Jang, S. Y. Kim and B. Yang, *Compos. Sci. Technol.*, 2019, **171**, 244–251.
13 H. Lee, D. Lee, J. Cho, Y. O. Kim, S. Lim, S. Youn, Y. C. Jung, S. Y. Kim and D. G. Seong, *Composites*, 2019, **123**, 108–113.
14 Z. Jundong, X. Renjie, Z. Fuxing, P. Tangping, H. Jiang, X. Le, X. Huasheng, W. Kang and J. Chongwen, *ACS Sustainable Chem. Eng.*, 2020, **8**, 71–83.
15 D. Hu, M. Zeng, Y. Sun, J. Yuan and Y. We, *SusMat*, 2021, **1**, 266–284.
16 J. Cao, Y. Cai, L. Yu and J. Zhou, *J. Mater. Chem. B*, 2019, **7**, 676–683.
17 M. Akter, M. Bhattacharjee, A. K. Dhar, F. B. A. Rahman, S. Haque, T. U. Rashid and S. M. F. Kabir, *Gels*, 2021, **7**, 1–28.
18 M. D. Luigi, Z. Guo, L. An, J. N. Armstrong, C. Zhou and S. Ren, *RSC Adv.*, 2022, **12**, 21213–21222.